Supporting Information

Dimethyl Sulfide Facilitates Acid Catalysed Ring Opening of the Bicyclic Monoterpenes in Crude Sulfate Turpentine to Afford *p*-Menthadienes in Good Yield

Joshua D. Tibbetts[a,b] and Steven D. Bull.[a]*

[a]Department of Chemistry, University of Bath, Bath, BA27AY, UK

[b]Centre for Sustainable Chemical Technologies, University of Bath, Bath, BA27AY, UK

E-mail: s.d.bull@bath.ac.uk

Contents

Table S1 Single step processes for transforming α-pinene, crude sulfate turpentine (CST), gum turpentine (GT) or 1,8-cineole into *p*-cymene.

Feedstock	Conditions	Yield of *p*-cymene	Yield of other products (if specified)	Ref
α-pinene	Faujasite Y, 300 °C, Tubular flow reactor, N_2	44%	*m*-Cymene (9%), *o*-Cymene (1%)	1
α-pinene	Mixed Zn/Cr oxide, 350 °C, N_2	78%	Camphene (4%), others (18%)	2
α-pinene	$H_3PW_{12}O_{40}$ on Si, 160 °C	68%	*p*-Menthenes (20%)	3
α-pinene	Pd/Zn on Al-SBA15, 300 °C, H_2	77%	Limonene, Camphene, *m*-Cymene and *p*-Menthene (% not specified)	4
α-pinene	H_2O, 400 °C, 300 bar, O_2	30%	Limonene (%not specified)	5
GT	H_2SO_4, Pd/C (0.2 wt%), 120 °C	62%	Not specified	6
GT	Ce/Pd doped AlSi-PENTA® SN-55, 300 °C, N_2	82%	Not specified	7
CST (65% α-pinene, 24% 3-carene, 11% others)	Faujasite Y, 300 °C, Tubular flow reactor, N_2	20%	*m*-Cymene (8%), *p*-MeDs (11%), *p*-Menthenes (16%), *p*-Menthanes (4%)	1
CST (65% α-pinene, 25% β-pinene, 10% others)	i) 5 wt% NaOCl pre-treatment ii) 0.1 wt% Pd on Si, 300 °C, 25% H_2 in N_2	65%	Bicyclic terpenes (30%), Monocyclic terpenes (5%)	8
1,8-cineole	Pd-doped γ-Al_2O_3	90%	Limonene	9

Table S2 Processes for transforming α-pinene or CST into mixtures of *p*-MeDs.

Feedstock	Conditions	Yield *p*-MeDs	Yield of other products (if specified)	Ref
α-pinene	NH_4-FER zeolite, 90 °C	Limonene (45%)	Camphene (40%)	10
α-pinene	Mordenite Y, 150 °C, 3 bar N_2	Dipentene (36%) Terpinolene (36%)	Camphene (4%)	11
α-pinene	Amorphous zirconium phosphate, 300 °C	Limonene (31%) α-terpinene (3%) γ-terpinene (10%) terpinolene (4%) isoterpinolene (10%)	*p*-Cymene (14%) Camphene (6%)	12
α-pinene	ZSM-5-NaOH, 150 °C, 6 bar N_2	Limonene (15%) α-terpinene (17%) γ-terpinene (7%) terpinolene (10%)	Camphene (34%)	13
α-pinene	TiO_2/WO_X, H_2O, 250 °C, 10 bar	α-terpinene (24%) γ-terpinene (8%) isoterpinolene (11%) terpinolene (1%)	Camphene (22%) Tricyclene (9%)	14
α-pinene	H_2O, MW (1.2 kW)	Limonene (14%) α-terpinene (12%) γ-terpinene (24%) terpinolene (20%)	Allocimene (9%)	15
CST (42% α-pinene, 12% β-pinene, 46% 3-carene)	$H_2SO_{4\,(aq)}$, 110 °C, 5 h	α-terpinene, γ-terpinene, terpinolene (76% total)	Polymeric material	16

Table S3 Palladium catalysed processes for transforming *p*-MeDs into *p*-cymene

Feedstock	Conditions	Yield *p*-cymene	Yield of other products (if specified)	Ref
Limonene (30%), Terpinolene (31%), α-terpinene (8%), γ-terpinene (6%), *p*-cymene (13%)	Pd/C, 300 °C, N_2	95%	*p*-Menthane (2%) *p*-Menthene (1%)	[17]
Limonene	Pd-HZSM-5, *n*-dodecane, 8 bar N_2 260 °C	82%	*p*-Menthane (16%)	[18]
α-terpinene	Pd/C (10%), 140 °C	82%	*p*-Menthane (18%)	[19]

Table S4 Non-palladium catalysed processes for transforming *p*-MeDs into *p*-cymene

Feedstock	Conditions	Yield *p*-cymene	Yield of other products (if specified)	Ref
Unspecified mixture of α-terpinene, γ-terpinene and terpinolene	$FeCl_3$ (0.24 eq.), water, *p*-cymene, 90 °C, 1.5 h	29%	Not specified	[16]
Limonene	Sodium (20 mol%), ethylenediamine (70 mol%), $FeCl_3$ (0.2%), 100 °C, N_2	99% (crude)	Not specified	[20]
Limonene	I_2 (0.5 equiv.), DDQ (0.5 equiv.), toluene, 110 °C	82%	Not specified	[21]
Limonene	Fe-modified sepiolite, MW, 180 °C	100%	-	[22]
α-terpinene	DMSO, 100 °C	88%	*p*-Methylacetophenone (10%)	[23]
γ-terpinene	DMF, 100 °C	95%	Not specified	[23]
γ-terpinene	Air (30 bar), 210 °C	82%	Terpinolene 8-Hydroxy-*p*-cymene (% not specified)	[24]
γ-terpinene	$H_4[PMo_{11}VO_{40}]$ (0.5 mol%), Diethyl carbonate, O_2, 70 °C	87%	Not specified	[25]
Terpinolene	$H_4[PMo_{11}VO_{40}]$ (0.5 mol%), Diethyl carbonate, O_2, 70 °C	71%	Not specified	[25]

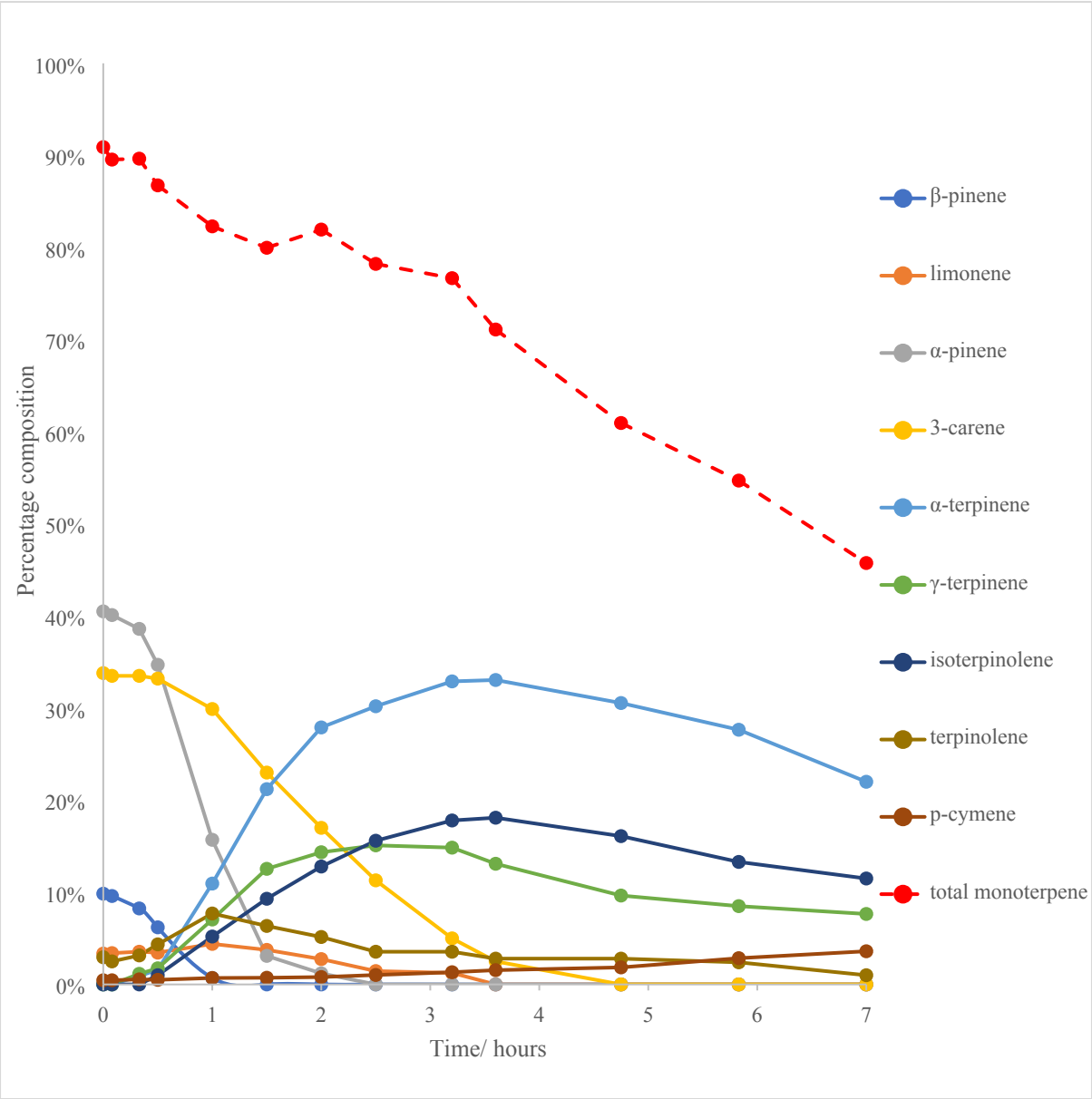

Figure S1 Time course of monoterpenes produced in the ACRO reaction of CST when treated with 6M $H_2SO_{4(aq)}$ at 90 °C.

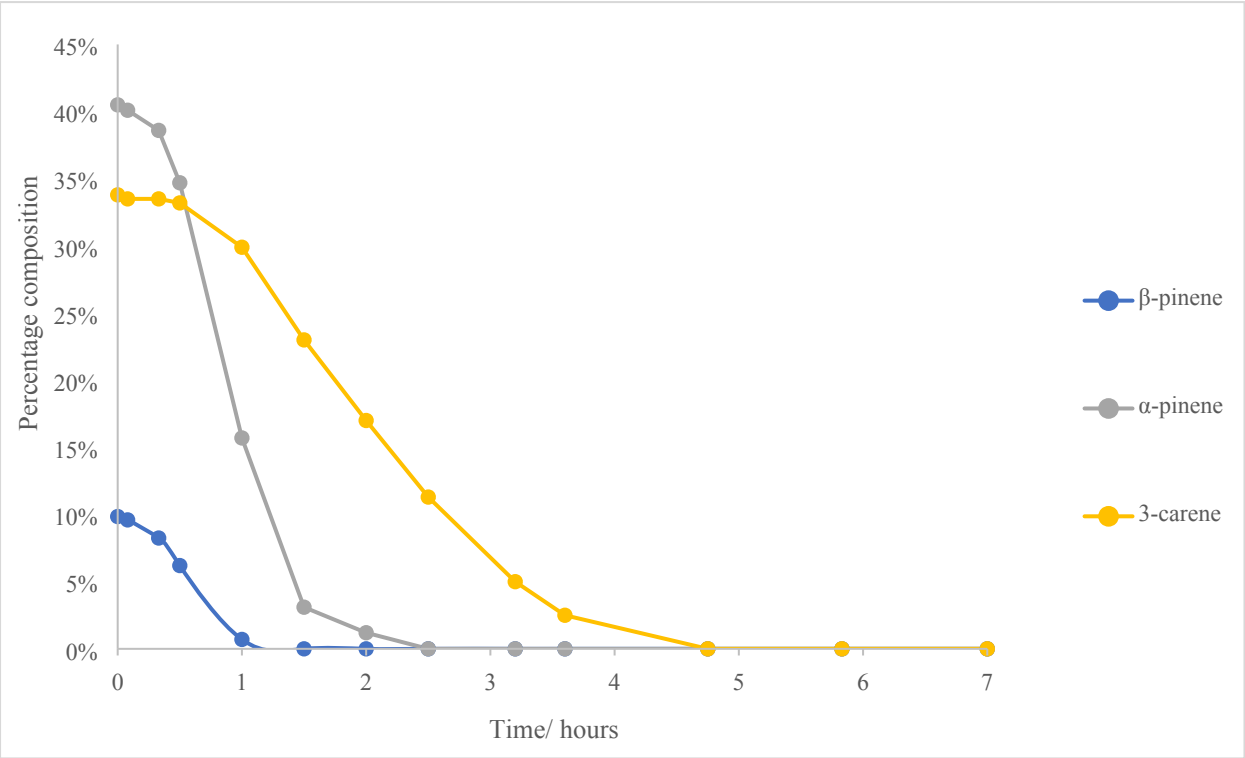

Figure S2 Time course of the consumption of bicyclic monoterpenes in CST when treated with 6M $H_2SO_{4(aq)}$ at 90 °C.

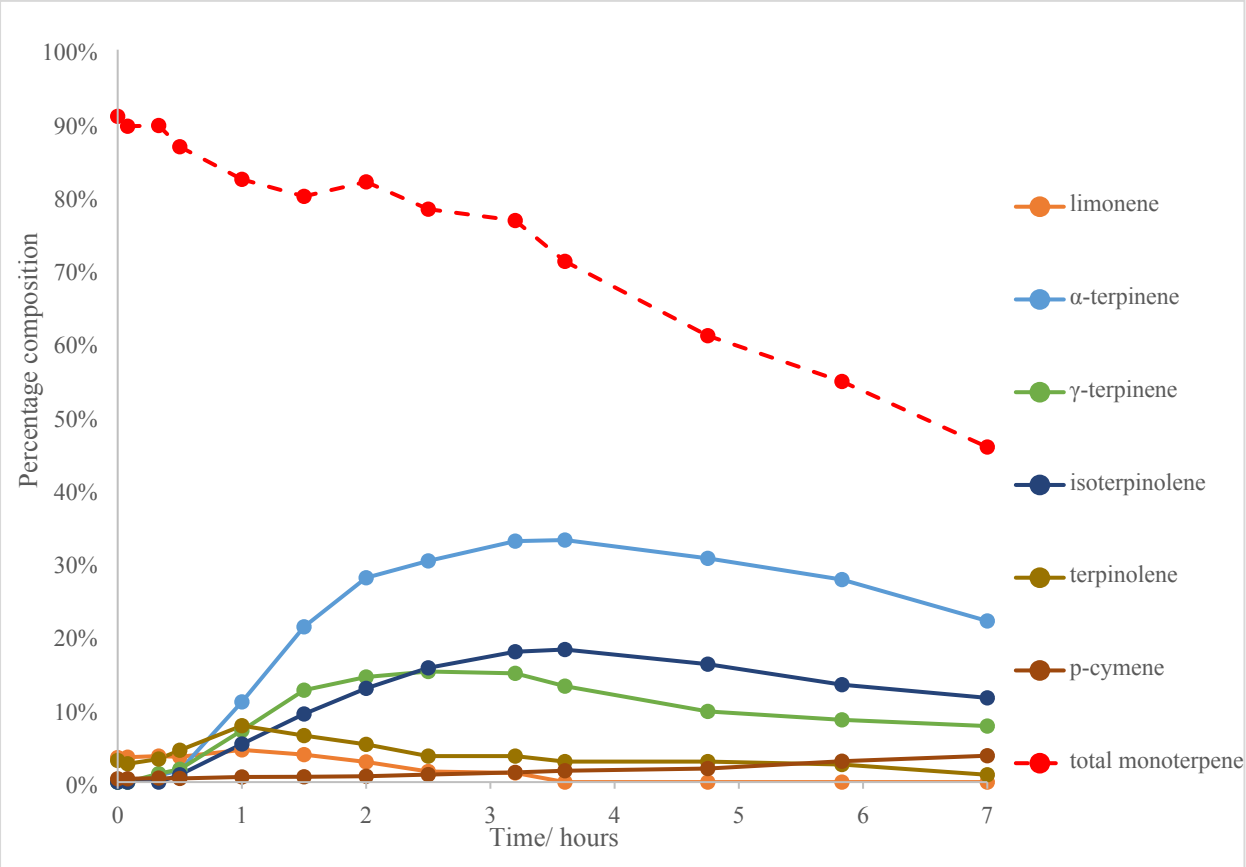

Figure S3 Time course of the ratio of *p*-MeDs produced when CST is treated with 6 M $H_2SO_{4(aq)}$ at 90 °C.

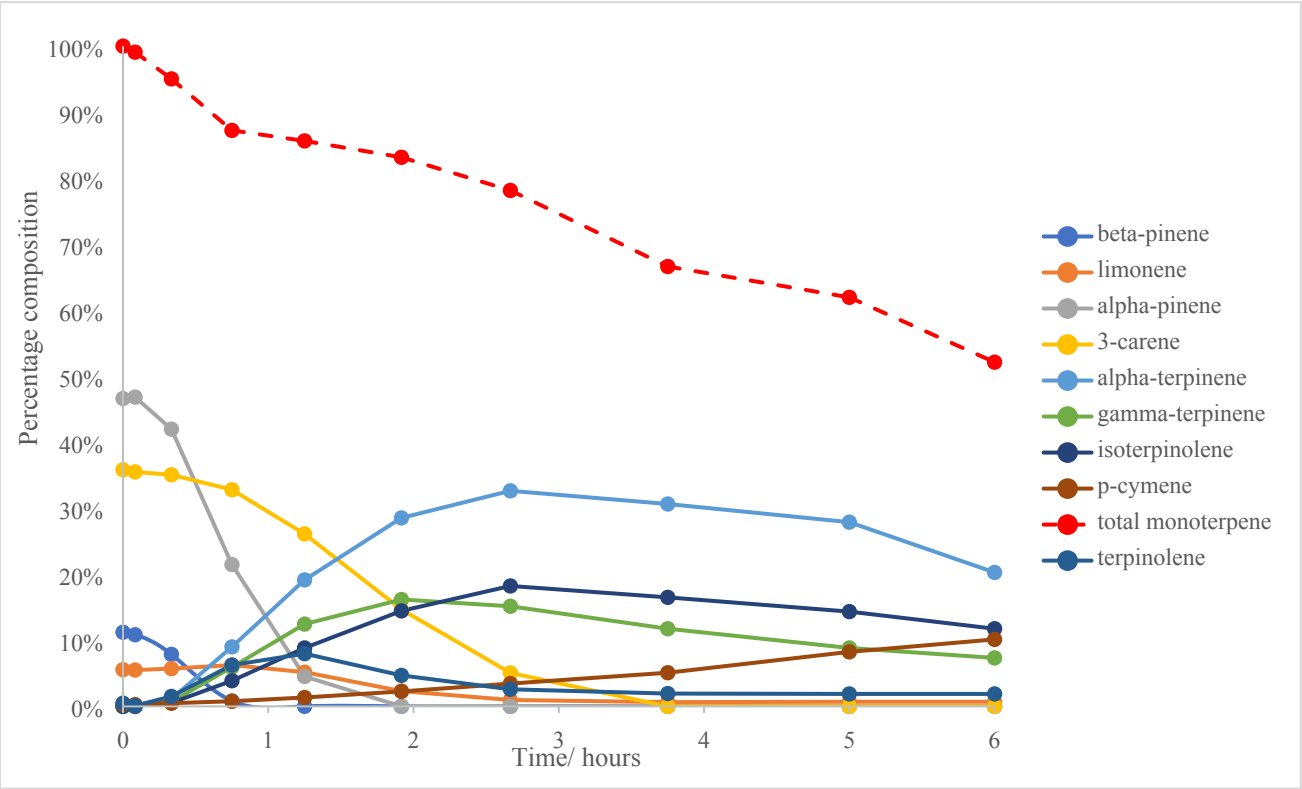

Figure S4 Time course of the ratio of *p*-MeDs produced when 'mock' CST is treated with 6M $H_2SO_{4(aq)}$ and 5 mol% Me_2S at 90 °C.

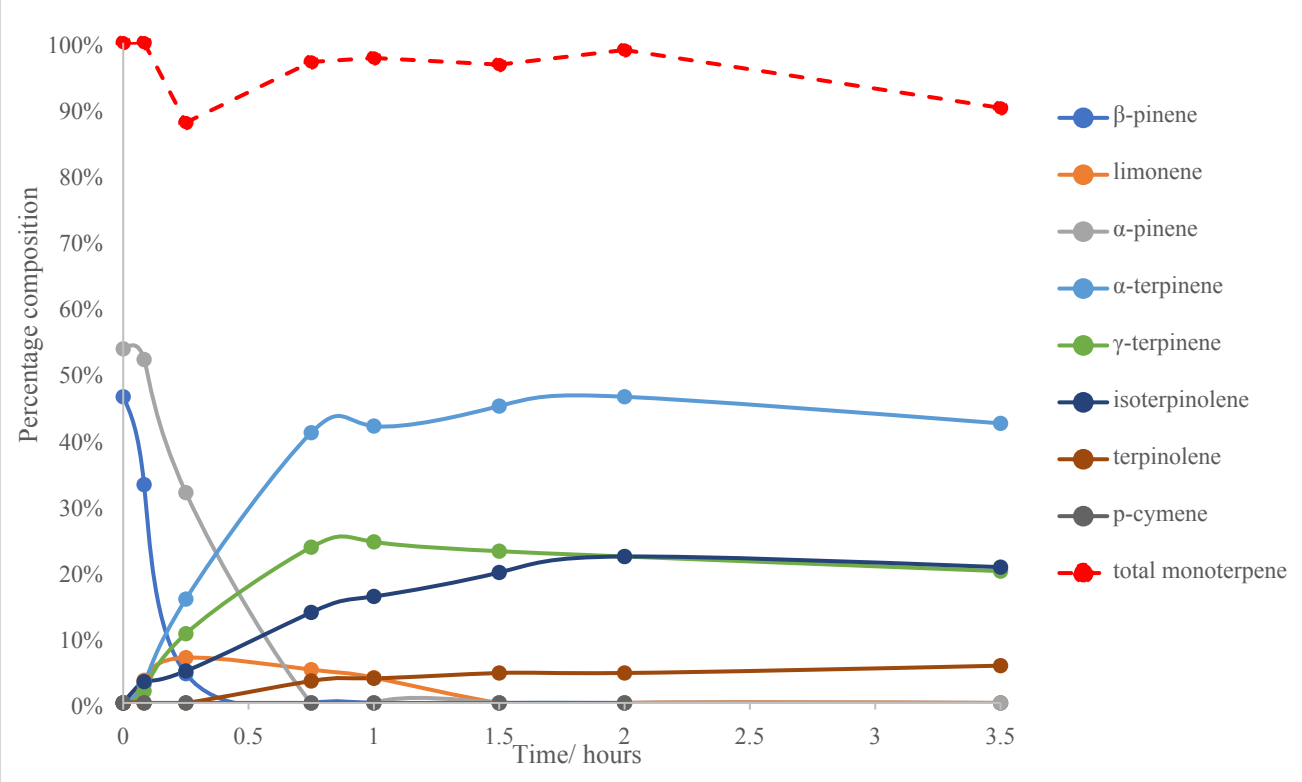

Figure S5 Time course of the ratio of *p*-MeDs produced when gum turpentine is treated with 6M $H_2SO_{4(aq)}$ and 5 mol% Me_2S at 90 °C.

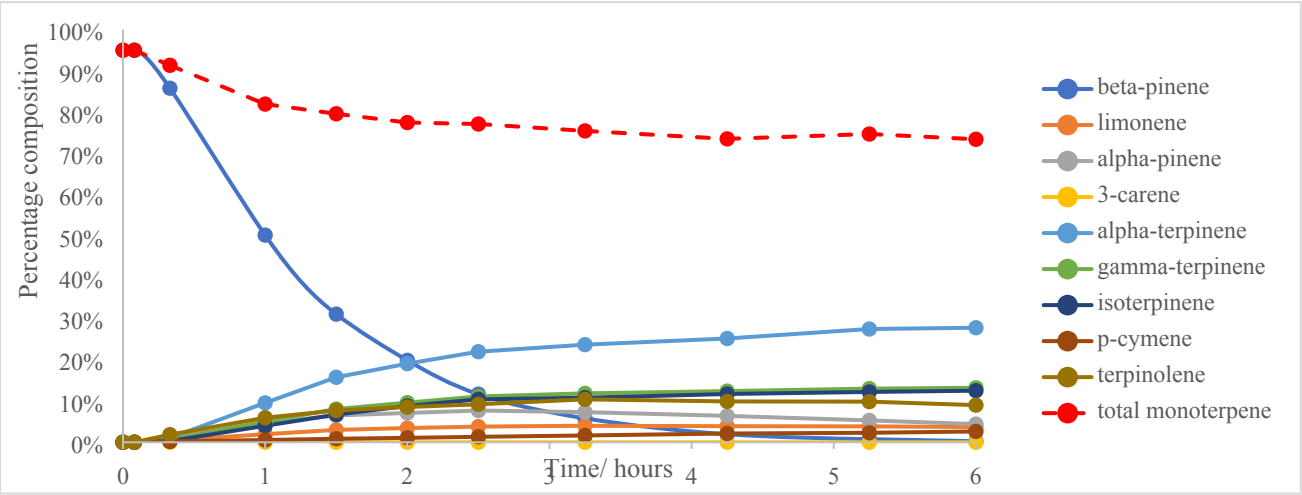

Figure S6 Time course of the ratio of *p*-MeDs produced when β-pinene is treated with 6M $H_2SO_{4(aq)}$ at 90 °C.

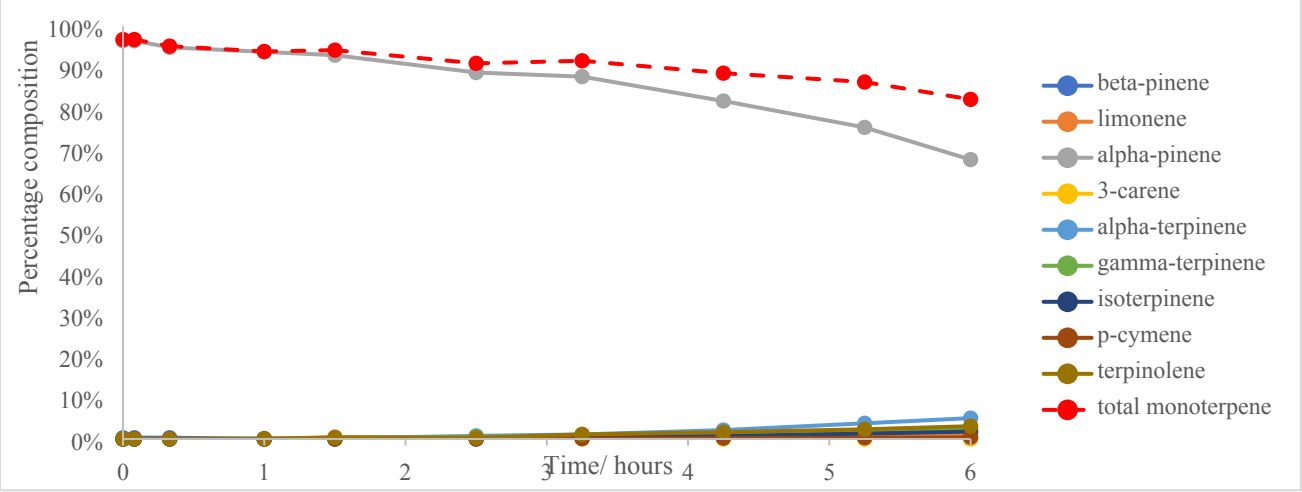

Figure S7 Time course of the ratio of *p*-MeDs produced when α-pinene is treated with 6M $H_2SO_{4(aq)}$ at 90 °C.

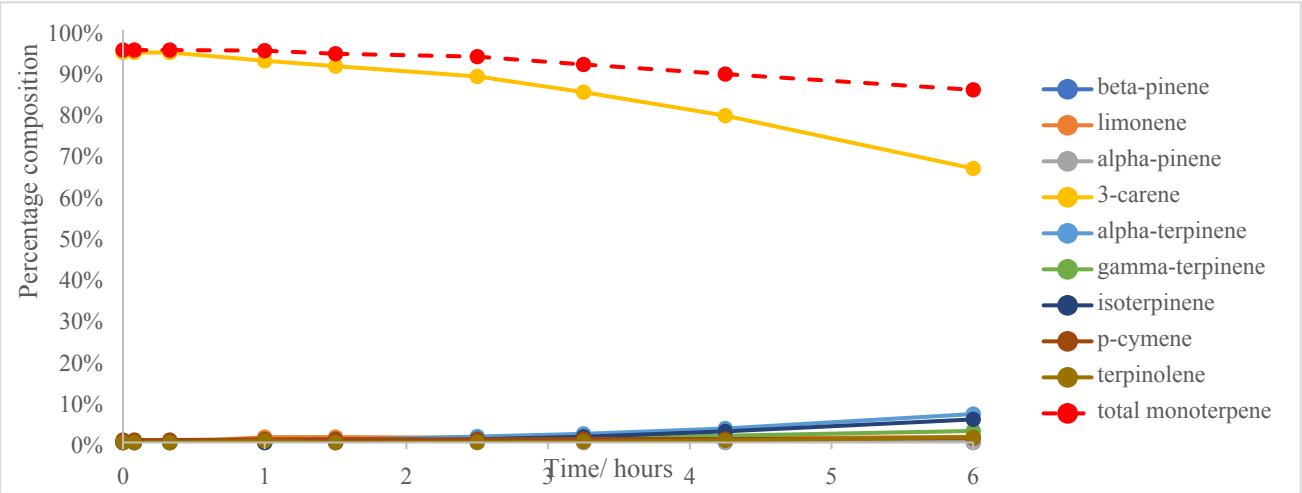

Figure S8 Time course of the ratio of *p*-MeDs produced when 3-carene is treated with 6M $H_2SO_{4(aq)}$ at 90 °C.

Table S5 Structures and ^{1}H NMR chemical shifts of the diagnostic alkene protons of the major bicyclic monoterpenes in CST and the *p*-MeD products produced in their ACRO reaction.

Compound	Structure	Chemical shift (ppm)
1,2,4,5-tetramethylbenzene	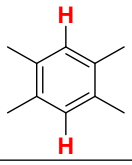	6.92 (**2H**)
α-pinene	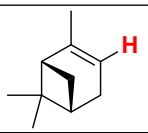	5.21 – 5.16 (**1H**)
β-pinene	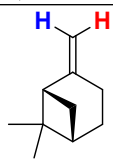	4.65 – 4.61 (**1H**) & 4.58 – 4.54 (**1H**)
3-carene	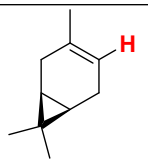	5.27 – 5.21 (**1H**)
Limonene	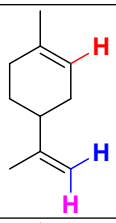	5.43 – 5.36 (**1H**) & 4.73 – 4.69 (**1H**+**1H**)
α-terpinene	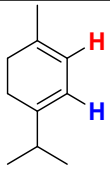	5.68 – 5.58 (**1H**+**1H**)
γ-terpinene	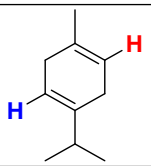	5.47 – 5.43 (**1H**+**1H**)
isoterpinolene	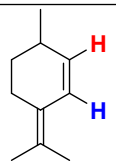	6.45 – 6.38 (**1H**) & 5.58 – 5.51 (**1H**)
terpinolene	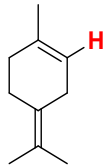	5.43 – 5.36 (**1H**)
p-cymene	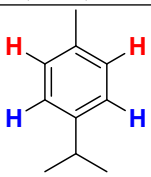	7.16 – 7.08 (**2H**+**2H**)

The internal standard (10 mol%) has two aromatic protons at δ_H 6.92 ppm and was set to an integral value of 2.00 in all NMR spectra (each proton integrating to 1). This means a single proton from any monoterpene integrating to 1 makes up 10 mol% of the organic terpene content.

Integrations for non-overlapping ^{1}H NMR proton resonances were measured wherever possible. In those cases where proton resonances for monoterpene **A** were overlapped with resonances from monoterpene **B**, then the integral value for monoterpene **A** was calculated by subtracting the integration value of a non-overlapping proton resonance for monoterpene **B** from the combined integrals of the overlapped **A**+**B** resonance.

For example, Figure S15 shows an overlapped signal at δ_H 5.70-5.50 ppm corresponding to both alkene proton resonances from α-terpinene and one alkene proton resonance from isoterpinolene which integrate to a total value of 8.36. The other alkene proton resonance for isoterpinolene appears with no overlap at δ_H 6.45 – 6.38 ppm, which integrated to 1.78. Consequently, the integral value for the two alkene protons of α-terpinene is calculated as: 8.36 – 1.78 = 6.58. This gives a value of 3.29 for each proton, meaning α-terpinene comprises 32.9% of the total monoterpene content.

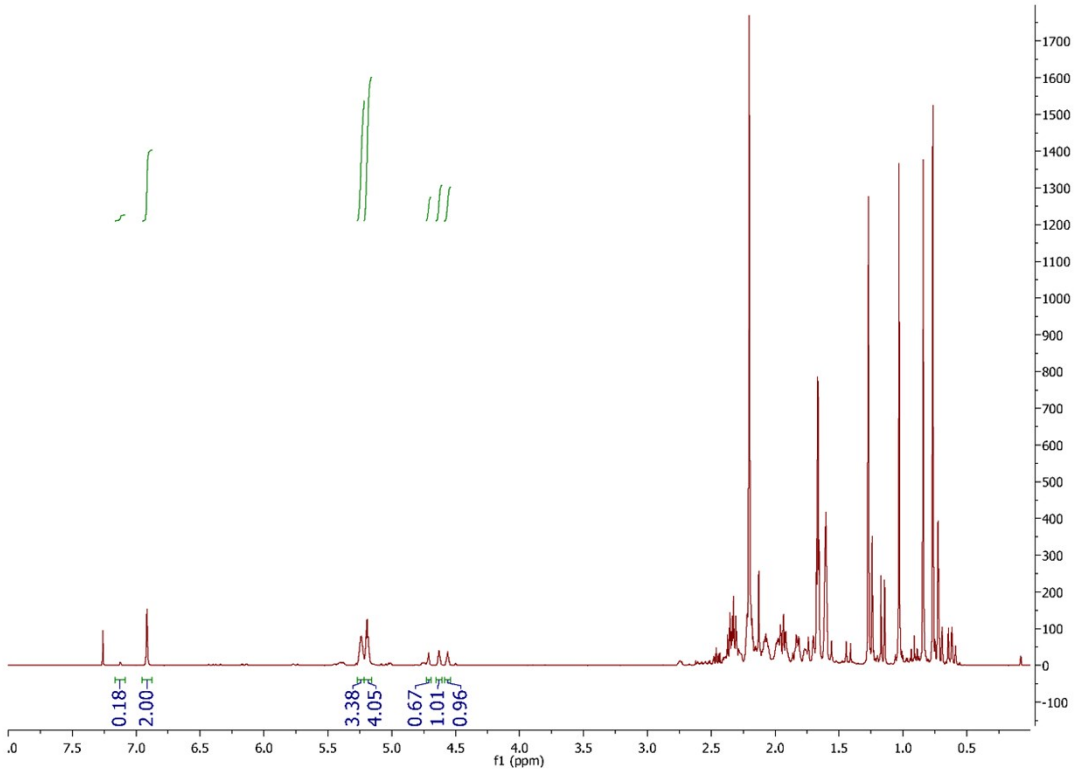

Figure S9 ^{1}H NMR spectrum of CST containing 1,2,4,5-tetramethylbenzene (10 mol% assuming a MW for CST of 136 gmol^{-1}) as an internal standard.

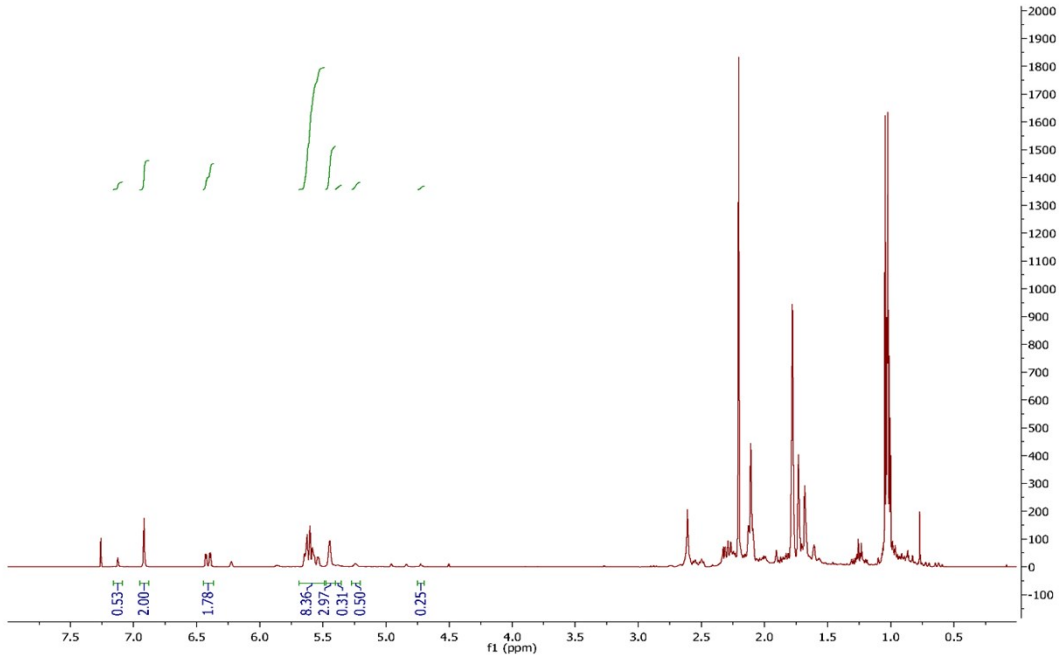

Figure S10 ^{1}H NMR spectrum of the monoterpenes produced in the ACRO reaction of CST after 3.25 h using 1,2,4,5-tetramethylbenzene (10 mol%) as an internal standard.

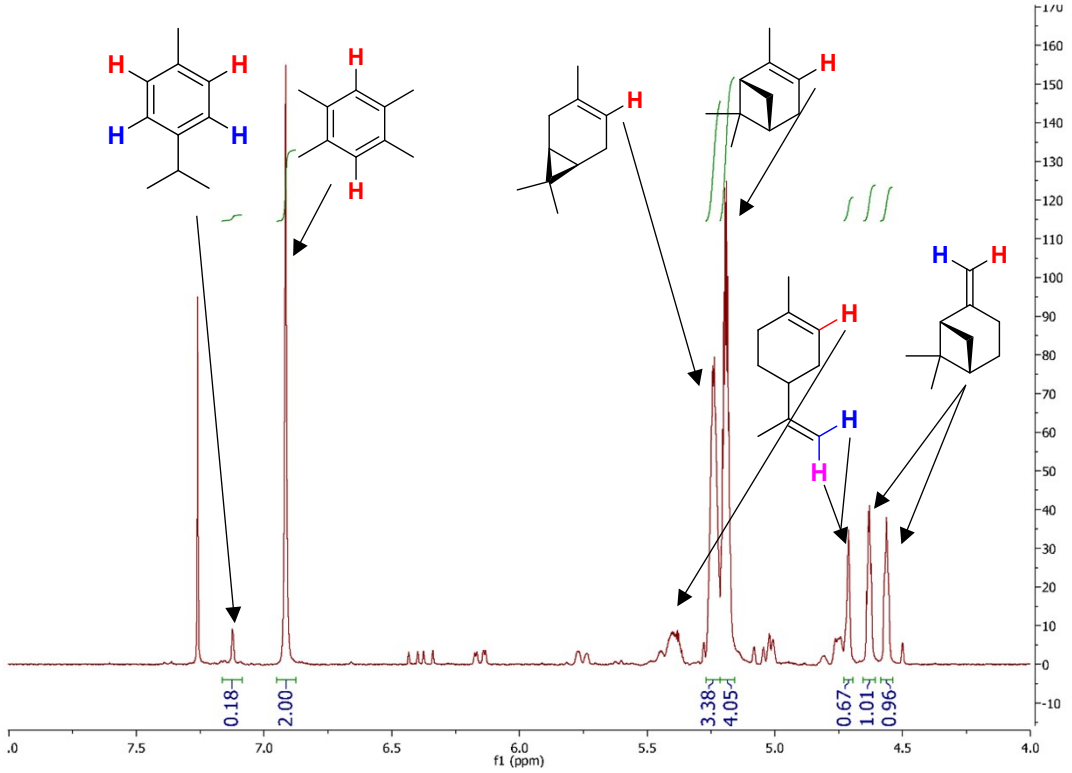

Figure S11 4.0 – 8.0 ppm region of the ^{1}H NMR spectrum of CST containing 1,2,4,5-tetramethylbenzene (10 mol%) as an internal standard.

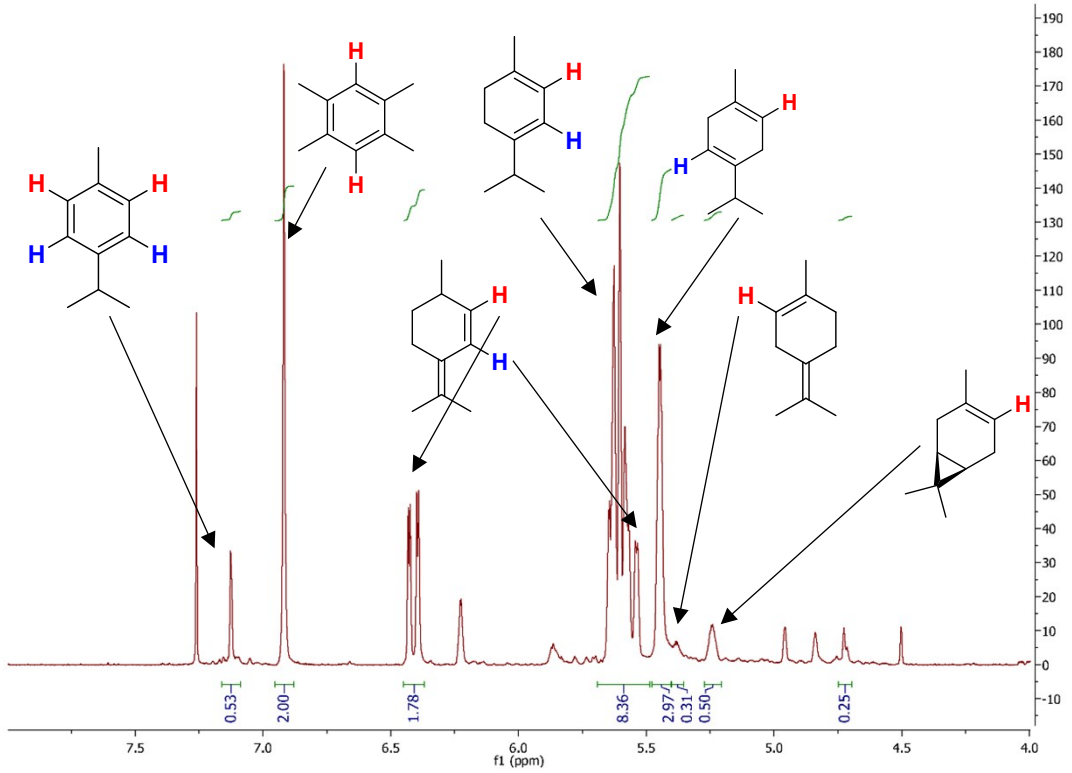

Figure S12 4.0 – 8.0 ppm region of the ^{1}H NMR spectrum of the reaction products produced in the ACRO reaction of CST after 3.25 h containing 1,2,4,5-tetramethylbenzene (10 mol%) as an internal standard.

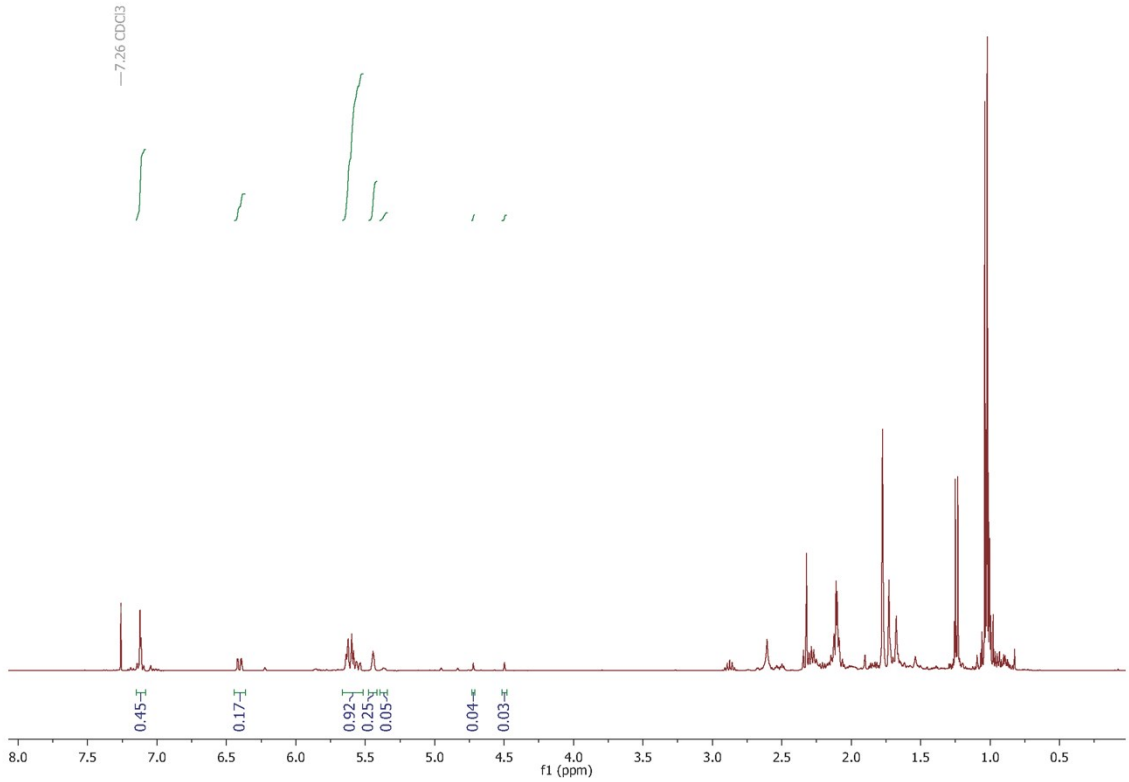

Figure S13 ^{1}H NMR spectrum of a distilled mixture of *p*-MeDs produced from an ACRO reaction of CST.

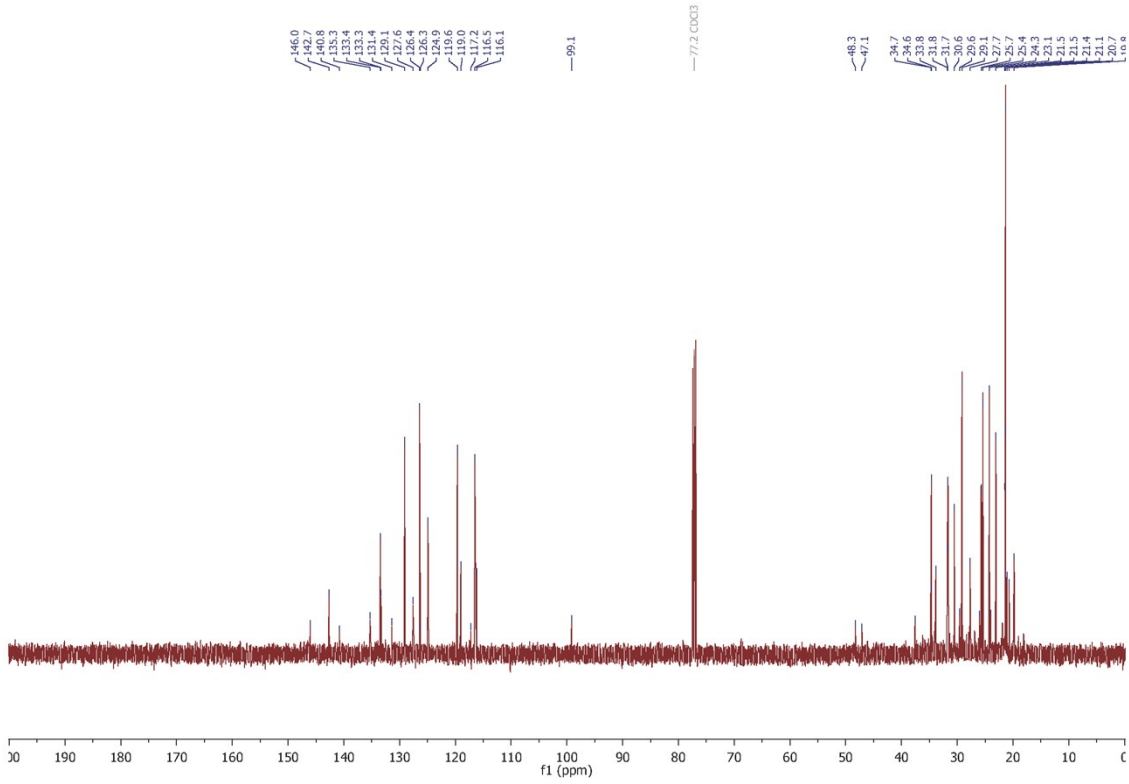

Figure S14 ^{13}C NMR spectrum of a distilled mixture of *p*-MeDs produced from an ACRO reaction of CST.

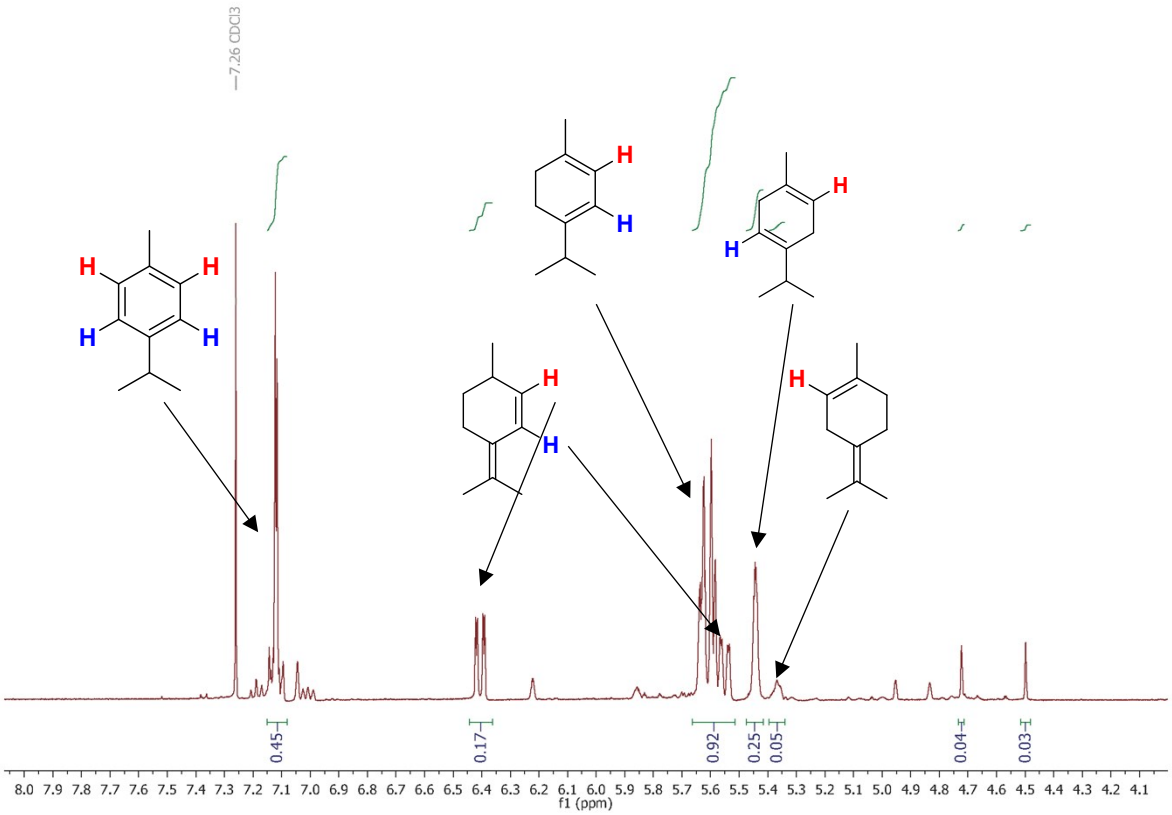

Figure S15 Expanded alkene region of ^{1}H NMR spectrum of distilled *p*-MeDs from the ACRO reaction of CST.

Procedure for preparing a mixture of 2-carene/3-carene

Anhydrous iron (III) chloride (0.023 g, 0.4 mmol) was added to ethylenediamine (3.3 mL, 49 mmol) and sodium metal (0.32 g, 14 mmol) under a N_2 atmosphere. The mixture was stirred at 50 °C until black spots began to form on the sodium surface, with the reaction mixture then heated to 95 °C to afford a bubbling black solution. 3-carene (9.52 g, 70 mmol) was then added dropwise over a period of 8 min. After stirring for 2 hours, the reaction was allowed to cool to room temperature before being quenched by the dropwise addition of water (25 mL). ^{1}H NMR spectroscopic analysis of the crude organic layer (8.02 g, 59 mmol, 84% yield) revealed that it was comprised of a mixture of 3-carene and 2-carene in a 56:44 ratio, as determined from integration of their characteristic alkene proton resonances at δ5.56 and δ5.25, respectively.[26]

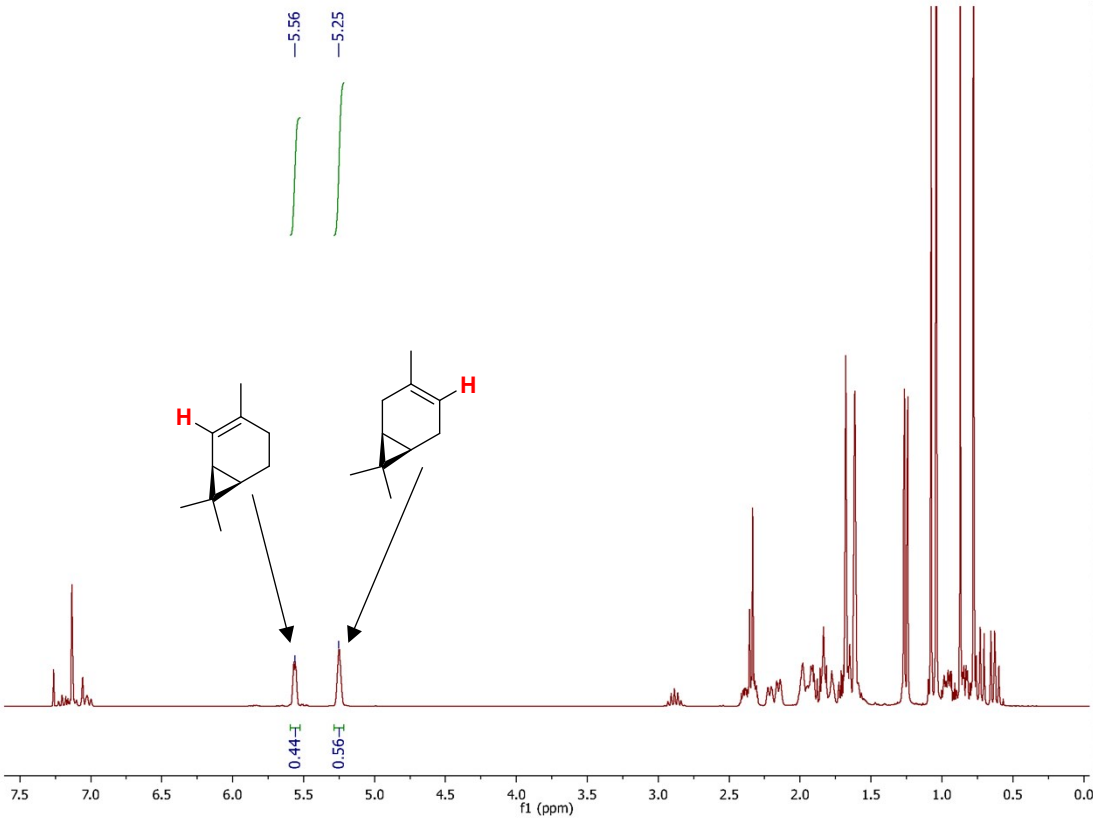

Figure S16 ^{1}H NMR spectrum of a 56:44 mixture of 3-carene and 2-carene.

High resolution mass spectrometric analysis was used to detect the presence of bicyclic monoterpenes, *p*-MeDs and monomeric/oligomeric terpene sulfonium species in both the aqueous and organic layers of the ACRO reaction. Aliquots of both layers were taken and diluted in acetonitrile, with direct injection then used to analyse the samples using a Bruker MaXis HD ESI-QTOF mass spectrometer. HRMS spectra are shown in comparison with calculated MS spectra displaying predicted isotopic patterns for comparative purposes.

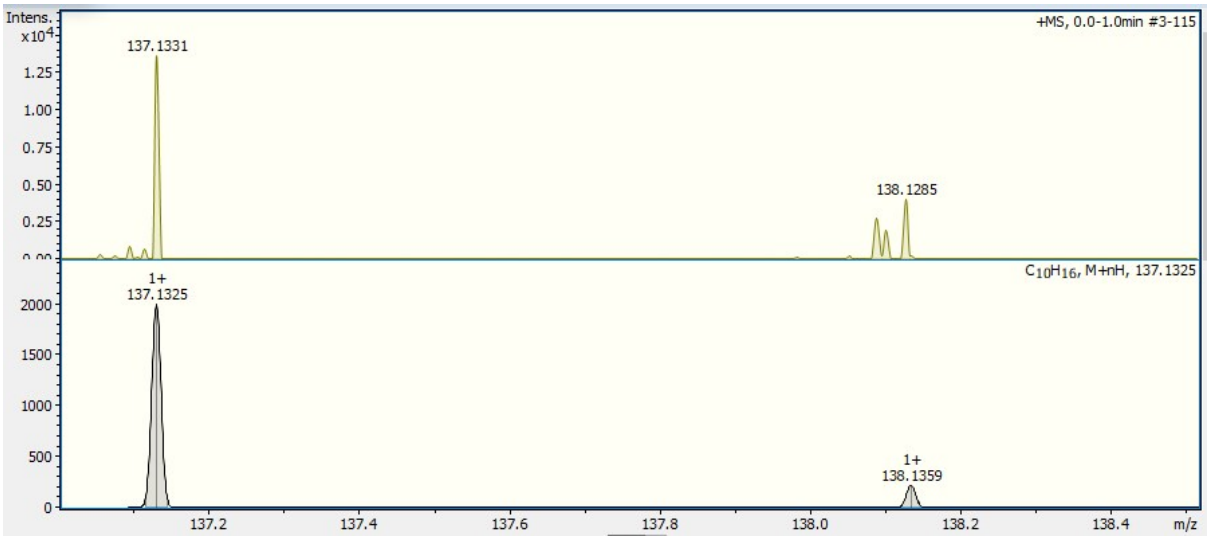

Figure S17 Top: High resolution mass spectrum showing a $C_{10}H_{17}^+$ peak at 137.1331 corresponding to $[M+H]^+$ for bicyclic monoterpene and/or *p*-menthene ions. Bottom: Predicted isotopic pattern expected for an $[M+H]^+$ molecular ion of $C_{10}H_{17}^+$.

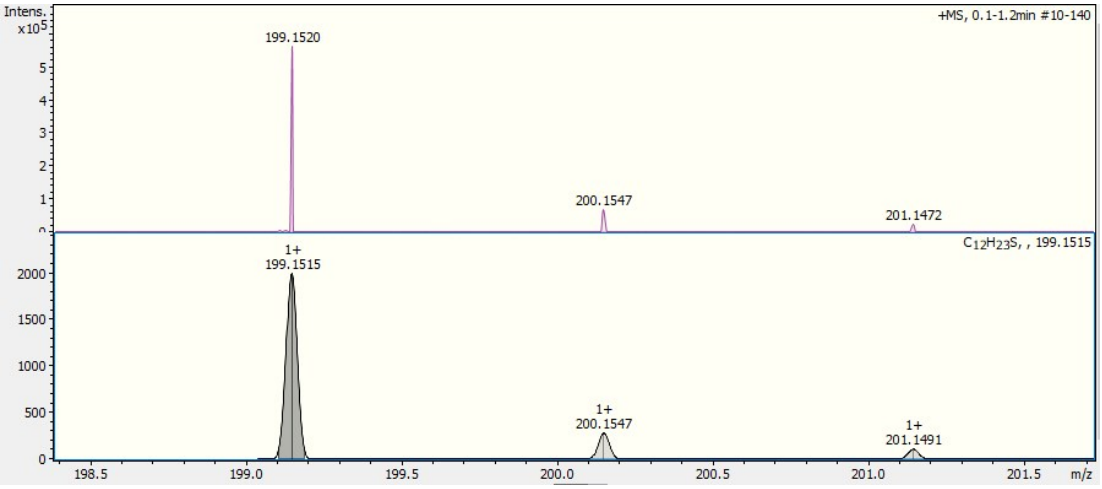

Figure S18 Top: High resolution mass spectrum showing a molecular ion peak at 199.1520 for a monomeric *p*-menthene sulfonium ion $C_{12}H_{23}S^+$. Bottom: Predicted isotopic pattern expected for the molecular ion of $C_{12}H_{23}S^+$.

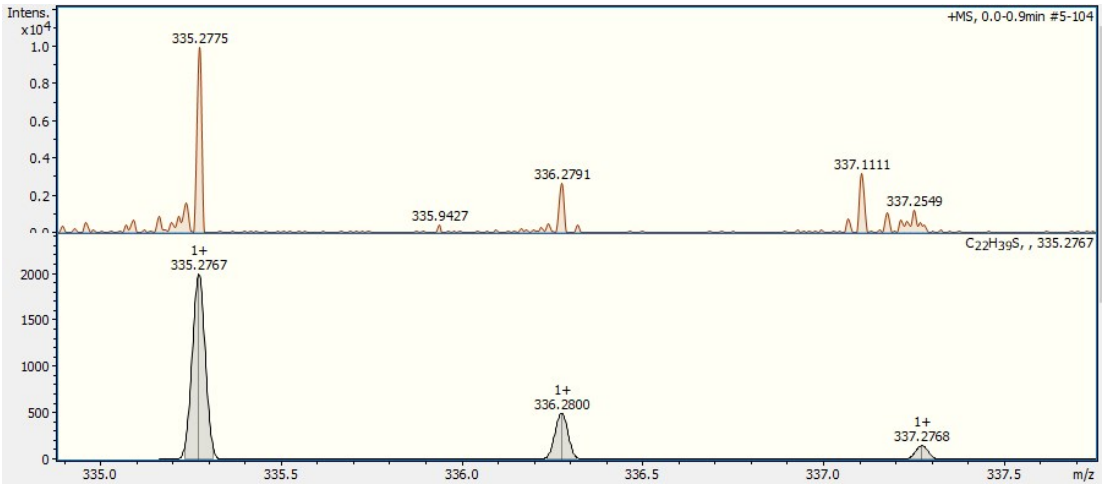

Figure S19 Top: High resolution mass spectrum showing a molecular ion peak at 335.2775 for a dimeric *p*-menthene sulfonium ion $C_{22}H_{39}S^+$. Bottom: Predicted isotopic pattern expected for the molecular ion of $C_{22}H_{39}S^+$.

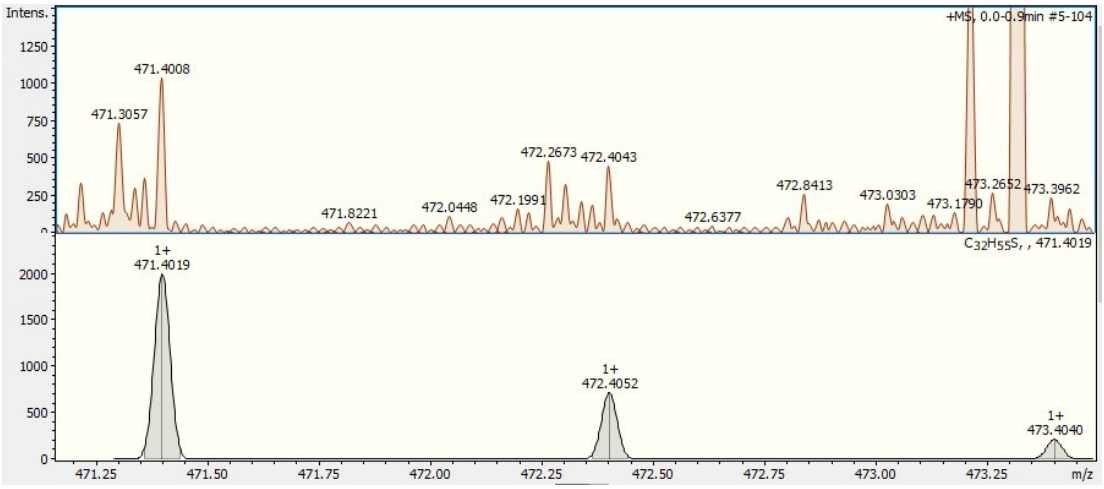

Figure S20 Top: High resolution mass spectrum showing a molecular ion peak at 471.4008 for a trimeric *p*-menthene sulfonium ion $C_{32}H_{55}S^+$. Bottom: Predicted isotopic pattern expected for the molecular ion of $C_{32}H_{55}S^+$.

References

1 J. A. Linnekoski, M. Asikainen, H. Heikkinen, R. K. Kaila, J. Räsänen, A. Laitinen and A. Harlin, *Org. Process Res. Dev.*, 2014, **18**, 1468–1475.

2 F. Al-Wadaani, E. F. Kozhevnikova and I. V. Kozhevnikov, *Appl. Catal. A Gen.*, 2009, **363**, 153–156.

3 H. Jaramillo, L. A. Palacio and L. Sierra, *Stud. Surf. Sci. Catal.*, 2002, **1**, 1291–1298.

4 M. Golets, S. Ajaikumar, M. Mohln, J. Wärnå, S. Rakesh and J. Mikkola, *J. Catal.*, 2013, **307**, 305–315.

5 T. Kawahara, Y. Henmi, N. Onda, T. Sato, A. Kawai-Nakamura, K. Sue, H. Iwamura and T. Hiaki, *Org. Process Res. Dev.*, 2013, **17**, 1485–1491.

6 L. Wang, X. Chen, X. Xu, X. Wei, L. Wang and Z. Tong, *Shipin Gongye Keji*, 2010, **31**, 197–199.

7 Hoechst AG, DE19521225A1, 1996.

8 D. M. Roberge, D. Buhl, J. P. M. Niederer and W. F. Hölderich, *Appl. Catal. A Gen.*, 2001, **215**, 111–124.

9 B. A. Leita, A. C. Warden, N. Burke, S. O. Shea and D. Trimm, *Green Chem.*, 2010, **12**, 70–76.

10 R. Rachwalik, M. Hunger and B. Sulikowski, *Appl. Catal. A Gen.*, 2012, **427**–**428**, 98–105.

11 A. I. Bokin, B. I. Kutepov, A. N. Khazipova, E. A. Travkin, N. A. Shchadneva, R. I. Khusnutdinov and U. M. Dzhemilev, *Russ. J. Appl. Chem.*, 2003, **76**, 234–237.

12 M. C. C. Costa, R. A. W. Johnstone and D. Whittaker, *J. Mol. Catal. A Chem.*, 1996, **104**, 251–259.

13 N. Nuttens, D. Verboekend, A. Deneyer, J. Van Aelst and B. F. Sels, *ChemSusChem*, 2015, **8**, 1197–1205.

14 M. Akizuki and Y. Oshima, *Ind. Eng. Chem. Res.*, 2017, **56**, 6204–6212.

15 T. Szuppa, A. Stolle and B. Ondruschka, *Org. Biomol. Chem.*, 2010, **8**, 1560–1567.

16 Holmen AB, WO/2015/023225/A1, 2015.

17 L. Bi, Q. Zhang, P. Wang, Z. Zhao, D. Li, Y. Chen, D. Li, Y. Gu, J. Wang and X. Liu, *Adv. Mater. Res.*, 2011, **238**, 27–34.

18 H. Cui, J. Zhang, Z. Luo and C. Zhao, *RSC Adv.*, 2016, **6**, 66695–66704.

19 J. H. Clark, E. M. Fitzpatrick, D. J. MacQuarrie, L. A. Pfaltzgraff and J. Sherwood, *Catal. Today*, 2012, **190**, 144–149.

20 M. Colonna, C. Berti, M. Fiorini, E. Binassi, M. Mazzacurati, M. Vannini and S. Karanam, *Green Chem.*, 2011, **13**, 2543.

21 V. Domingo, C. Prieto, L. Silva, J. M. L. Rodilla, J. F. Quílez Del Moral and A. F. Barrero, *J. Nat. Prod.*, 2016, **79**, 831–837.

22 M. A. Martin-Luengo, M. Yates, E. S. Rojo, D. Huerta Arribas, D. Aguilar and E. Ruiz Hitzky, *Appl. Catal. A Gen.*, 2010, **387**, 141–146.

23 H. Iwamuro, T. Ohshio and Y. Matsubara, *Nippon Kagaku Kaishi*, 1978, 909–911.

24 M. Asikainen, O. Jauhiainen, O. Aaltonen and A. Harlin, *Green Chem.*, 2013, **15**, 3230–3235.

25 Shanghaitech Univ, CN107008499 (A), 2017.

26 J. E. Cabaj, J. M. Lukesh, R. J. Pariza and P. M. Zizelman, *Org. Process Res. Dev.*, 2009, **13**, 358–361.